STUDY OF DIFFERENT MEMBRANE SPARGERS USED IN WASTE WATER TREATMENT: CHARACTERISATION AND PERFORMANCE

Pisut PAINMANAKUL[1], Karine LOUBIERE[1], Gilles HEBRARD[1] and P. BUFFIERE[2]

*[1]**L**aboratoire d'**I**ngénierie des **P**rocédés de l'**E**nvironnement, Département G.P.I.,*

Institut National des Sciences Appliquées,

135 avenue de Rangueil, 31077 Toulouse Cedex 4, France

[2]ONDEO Degrémont, CERDEG, 87, Chemin de Ronde, 78290 Croissy sur Seine, France

Abstract

In urban waste water treatment, a novel gas sparger based on flexible rubber membrane has been used for the last ten years. The objective of this present work is to compare two flexible membranes (the new membrane and the old membrane provided by ONDEO-DEGREMONT group) used in waste water treatment. For this purpose, the different membrane properties (hole diameter, pressure drop, critical pressure, deflection at the centerline and elasticity) have been characterized. The bubble generation at the membranes with a single orifice and with four orifices have been studied and their performances have been compared in terms of interfacial area and power consumption. From the experimental and theoretical approach, the new membrane is less elastic (or more rigid) than the old membrane. The bubble diameters generated from the new membrane remain constant with the gas velocity through the orifice, whereas they increase logarithmically for the old membrane. The inverse behaviours are observed in terms of the bubble formation frequency. Moreover, the bubbles generated from the new membrane have significantly larger sizes and lower formation frequencies than those obtained with the old one. From these results, it can be noted that the new membrane has a behaviour comparable to a rigid orifice. No coalescence phenomenon at the bubble formation is observed from the new and the old membranes with four orifices. The interfacial area and

the power consumption are evaluated and show slight differences between the interfacial area provided by the old and the new membranes for one value of power consumption.

Keywords : Waste water treatment; Flexible rubber membrane; Bubble generation; Bubble diameter; Bubble formation frequency; Interfacial area; Power consumption.

1. INTRODUCTION

In urban waste water treatment, for nitrification and for denitrification, the aeration of the biological process is essential to the micro-organism metabolism, and so to the consumption of the organic water pollution. The gas is released in the form of small bubbles to yield a large surface for mass transfer. With punctured flexible rubber membranes, uniform size distribution of small bubbles is produced leading to large mass transfer area [1], without the usual clogging problems encountered with a porous disk diffuser. Several works have been carried out on the membrane characterization (physical properties) and on the bubbles generated at the flexible orifice [2-5]. Hébrard et al. [6] and Couvert et al. [7] have indicated that the size of the bubbles generated from the membrane is determined at the moment of detachment and appears to be maintained afterwards in the reactor in non coalescent liquid. It is likely the small size of these bubbles, would render them stable to coalescence and breaking phenomena. However, no precise methods are available for comparing several membranes and for evaluating their performances.

The objective of this present study is to compare two flexible membranes used in urban waste water treatment by ONDEO-DEGREMONT company. The following membrane comparison techniques are proposed:

- Characterization of the physical membrane properties (hole diameter, pressure drop, critical pressure, deflection at the centerline and elasticity) by the experimental or theoretical approach.
- Characterization of the bubble diameter generated from the membranes and the associated bubble formation frequency.
- Evaluation of the interfacial area and the power consumption to compare the membrane performances.

In this study, the old and the new membranes with a single orifice are firstly studied in terms of the physical membrane properties and their bubble generation. Secondly, both these membranes with four orifices are characterized to have a better understanding of the behaviour of the membranes with multi orifices. Finally, the interfacial area and the power consumption are evaluated for the membranes with a single orifice and with four orifices to compare their performances.

2. EXPERIMENTAL SET-UP AND METHODS

2.1 EXPERIMENTAL SET-UP

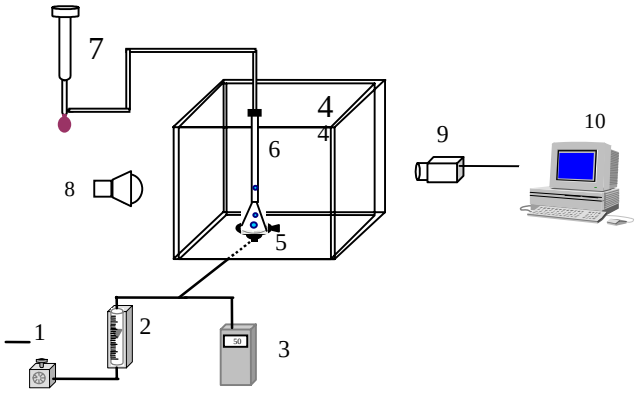

1 Pressure gauge
2 Gas flow meter
3 Electronic manometer
4 Bubble generation vessel
5 Membrane clamp
6 Funnel
7 Soap film meter
8 Halogen Lamp
9 Video camera
10 Acquisition computer

Figure 1: Schematic diagram of the experimental set-up

The experimental set-up is shown in figure 1. The experiments are carried out in a glass parallelepiped vessel (4), 0.40 m in width, 0.40 m in length, 0.30 m in height. The flow of air is monitored by a pressure gauge (1) and regulated by a gas flow meter (2). The membrane sparger is assembled on a circular clamping ring (5) composed of two jaws; this fixing system coupled with the use of a dynamometric spanner (0-5 Nm) enables the same initial tension to be applied, thus giving reproducible results whatever the membrane. The pressure drop created by the membrane is determined using an electronic manometer type BIOBLOCK 915PM247 (3). The average gas flow rate is measured using a soap film meter (7), through a funnel (6) put on the clamp. Tap water is used as the liquid phase (σ_L = 71.8 N/m, μ_L = 10.002 $.10^{-4}$ Pa.s, ρ_L=997 kg/m^3). The operating conditions are as follows: liquid height H_L = 20 cm, gas chamber volume V_C = 107-111 cm^3 and temperature condition T = 20 ^oC.

2.2 MEMBRANE SPARGERS

Two types of flexible membrane spargers are studied: the old membrane called O and the new membrane called N. Both have been provided by ONDEO-DEGREMONT Company. In this work, pieces of 60 mm diameter have been used. The bubbles are generated from a single orifice located at the membrane centre, or from four neighbouring orifices located at the membrane pole, or from the complete set of orifices. As punctures were initially distributed over the entire surface sheet, it was necessary in some cases to close several holes without modifying the elastic membrane properties; for this purpose, a silicone elastomer glue applied on the inner surface (gas chamber side) was used. The thickness of all membranes was 2.06 mm. Table 1 describes the membrane designation.

Name	**Property**
N1	Single orifice new membrane

O1	Single orifice old membrane
N4	Four orifice new membrane
O4	Four orifice old membrane
N	Multi orifice new membrane
O	Multi orifice old membrane

Table 1: Membrane designation

2.3 IMAGE ACQUISITION AND TREATMENT SYSTEMS

The detached bubbles are photographed with a Leutron LV95 camera (360 images/s). Images are visualised on the acquisition computer through the Leutron vision software. The measurements of membrane deflections at the centreline are also performed by this acquisition system.

Without liquid phase, the hole diameter measurements are based on the joint use of a Sony DXC 930P 3CCD Colour camera and a Nikon SMZ-U microscope. The image treatment is performed with the Visilog 5.4 software (C^{++} program).

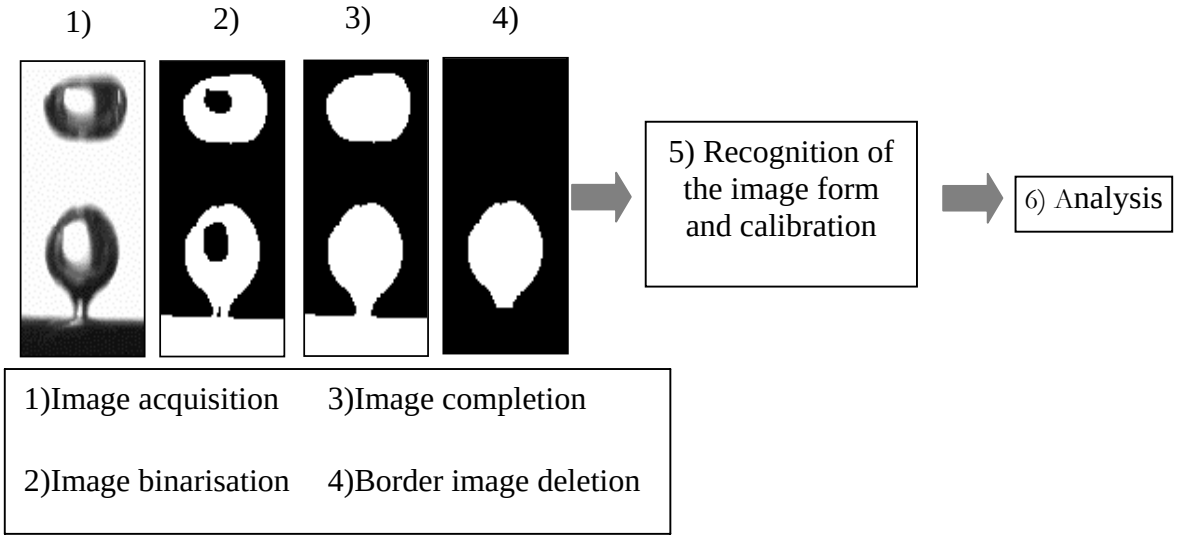

Figure 2: Typical sequence of the image treatment

Figure 2 presents a typical sequence of the image treatment. This treatment is based on a transformation of the acquired image into a binary image, followed by different arithmetical and geometrical operations. Then, the images are given uniform surface treatment and superfluous images are removed. As a result, the equivalent bubble (or hole) diameters are determined. The bubble frequency is deduced from photographic analysis by the number of associated images. If the configuration of the camera is 360 images/s, an image is acquired every 2.78 ms.

2.4 CALCULATION OF THE BUBBLE FORMATION FREQUENCY

Two methods are used to determine the bubble formation frequency:

a. The image treatment method (f_B)

Loubière [8] has defined the total bubble formation time (T_B) as:

$$T_B = T_{Growing} + T_{Out} \tag{1}$$

T_{out} is the time-out between two consecutive bubbles generated, it is equal to 0 with the flexible membrane (continuous process). $T_{Growing}$ is the time of the bubble growth. The bubble formation frequency is deduced from the total time formation (T_B) by Eq. (2):

$$f_B = \frac{1}{T_B} \tag{2}$$

b. The calculating method (f_{B1})

The bubble formation frequency which is the number of bubbles formed at the membrane orifice per unit time can be also calculated by:

$$f_{B1} = \frac{q}{V_B} \tag{3}$$

V_B is the mean detached bubble volume and q is the mean gas flow rate through each orifice, assuming uniform flow distribution, and is presented as Eq. (4):

$$q = \frac{Q_G}{N_{OR}} \tag{4}$$

Q_G is the gas flow rate entering the reservoir and N_{OR} is the number of orifices located on the membrane. If the distance between two orifices is sufficiently large, coalescence cannot occur during the bubble formation, so the bubble formation frequency is expressed as Eq. (5):

$$f_{B1} = \frac{N_{OR} \times q}{V_B} \tag{5}$$

c. Comparison of the two methods

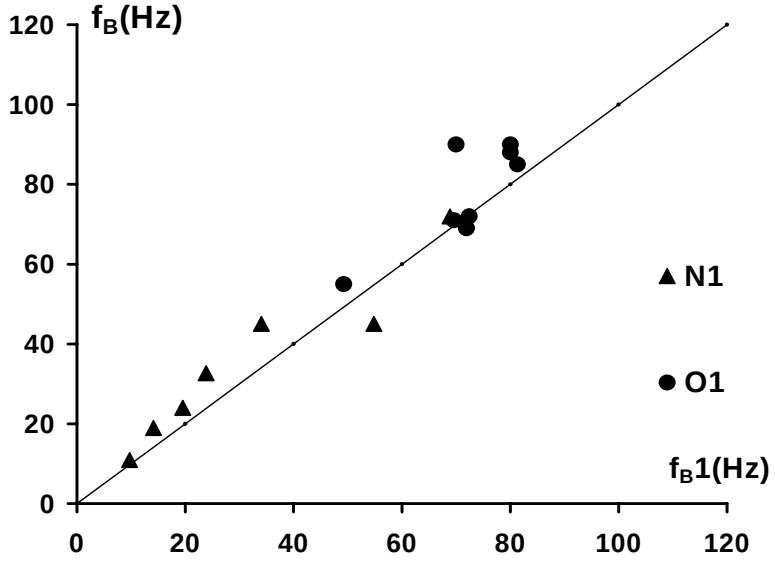

Figure 3: Comparison of the two methods for calculating the bubble formation frequency for the membranes with a single orifice

Figure 3 shows the comparison of the two methods for determining the bubble formation frequency. The results of the two methods are in quite good agreement: an average difference of 30% which corresponds to experimental error is observed.

2.5 CALCULATION OF THE INTERFACIAL AREA

The interfacial area (a) is one of the most important parameters in the study of the gas-liquid mass transfer in the reactor. It is defined as the ratio between the bubble surfaces (S_B) and the total volume in reactor (V_{Total}). The number of bubbles (N_B) is calculated from the terminal rising bubble velocities (U_B) and the bubble formation frequency (f_B):

$$N_B = f_B \times \frac{H_L}{U_B} \tag{6}$$

The velocities U_B are determined by using the experimental curves of Grace & Wairegi [9]. Consequently, the interfacial areas are expressed as Eq. (7):

$$a = N_B \times \frac{S_B}{V_{TOTAL}} = f_B \times \frac{H_L}{U_B} \times \frac{\pi . D_B^2}{A.H_L + N_B.V_B} \tag{7}$$

H_L and A are the liquid height (H_L = 0.20 m) and the cross-sectional area (A = 0.16 m^2) respectively. The ratio of the interfacial area associated with two membranes can be deduced as Eq. (8):

$$\frac{a_1}{a_2} \approx \frac{f_{B1}}{f_{B2}} \times \frac{U_{B2}}{U_{B1}} \times \frac{D_{B1}^2}{D_{B2}^2} \tag{8}$$

According to Eq. 8, the interfacial area is a function of the bubble formation frequency, the terminal bubble rising velocity and the detached bubble diameter.

2.6 CALCULATION OF THE POWER CONSUMPTION

In the case of a gas-liquid reactor equipped with membrane sparger in which mixing is induced pneumatically, the total specific power consumption (P_g/V_{Total}) can be related to the total gas pressure drop according to the following equation [10]:

$$\frac{P_G}{V_{Total}} = Q \times \frac{\Delta P_{Total}}{V_{Total}} = Q \times \frac{(\rho_L . g . H_L + \Delta P)}{V_{Total}} \tag{9}$$

With a membrane sparger, the total gas pressure drop (ΔP_{Total}) is a function of the liquid height ($\rho.g.H_L$) and of the specific sparger pressure drop (ΔP) which increases with the gas velocity through the orifice.

3. COMPARISON OF THE SINGLE ORIFICE MEMBRANES

3.1 CHARACTERISATION OF THE MEMBRANE WITH A SINGLE ORIFICE

a. Equivalent hole diameter.

The rubber membrane dynamic properties were studied experimentally. The image acquisition system previously described was used to measure the hole diameters. They correspond to the equivalent diameters defined from the area assuming a circular hole, given by Eq. (10):

$$D_{OR} = \left[\frac{4.(Hole \quad Area)}{\pi} \right]^{1/2} \tag{10}$$

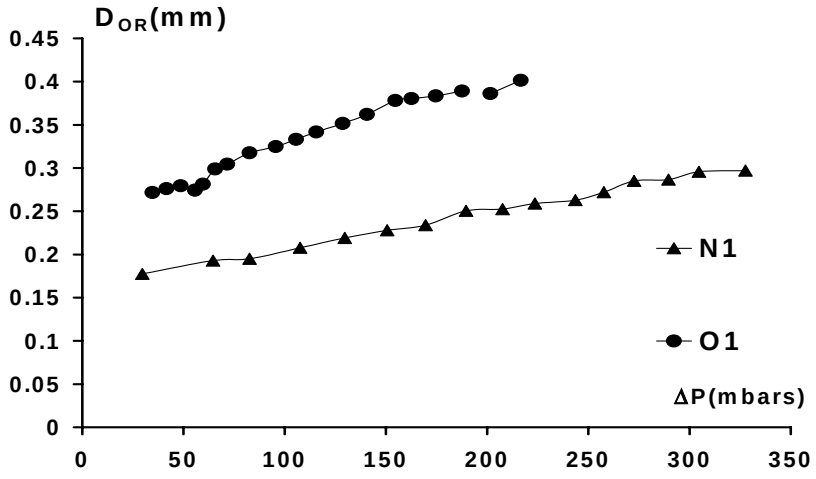

Figure 4: Equivalent hole diameter versus applied pressure for the membranes with a single orifice

Figure 4 shows that for a given ΔP, the hole diameter of the N1 membrane is about two times lower than that of the O1 membrane. For all the membranes, the apparent equivalent hole diameter increases with the applied pressure: when the pressure increases, the hole expands owing to the membrane's elastic nature. In this work, the hole diameter has been used to determine the gas velocity through the orifice U_G as Eq. (11):

$$U_G = \frac{Q_G}{N_{OR}.A_{OR}} = \frac{4.Q_G}{N_{OR}.\pi.D_{OR}^2} \tag{11}$$

Q_G is the gas flow rate entering the reservoir. N_{OR} is the number of orifices located on the membrane and A_{OR} is the hole area.

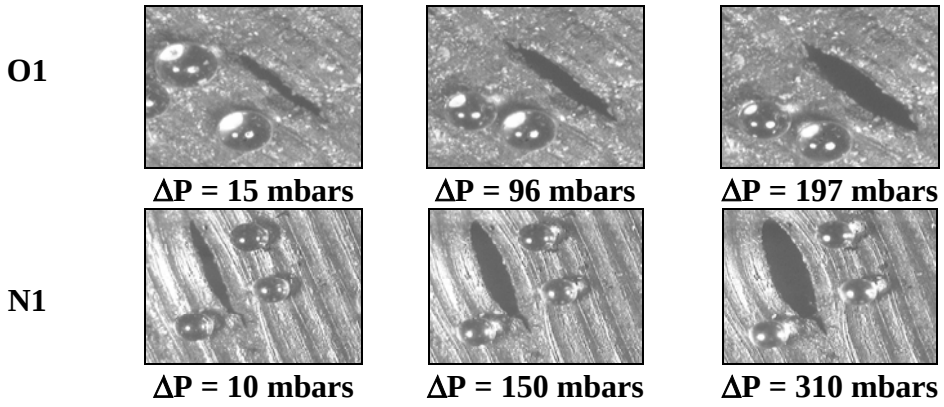

Figure 5: Hole photographs (calibration: glass particle 300 μm. in diameter)

The orifice varies in shape: at low applied pressures, the orifice appears as a slit and as the pressure increases, the slit expands to form a more circular shape (Figure 5).

b. Relation between the applied pressure drop and the gas flow rate

Loubière & Hébrard [5] observed a hysteresis when comparing the pressure at increasing and decreasing gas flow rates. In this paper, the authors have chosen to present results as the gas flow decreases.

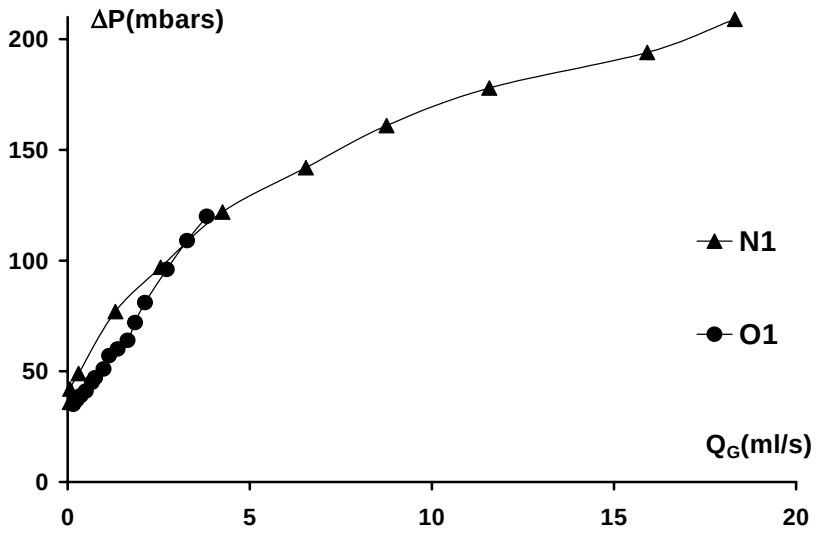

Figure 6: Applied pressure drop versus gas flow rate for the membranes with a single orifice

Figure 6 presents the experimental curves relating the applied pressure drop to the gas flow rate for the membranes (N1 and O1). Regardless of the membranes type, the applied pressure increases less than linearly with the gas flow rate. Nevertheless, some differences appear between the membranes: for a given Q_G, the applied pressure for the O1 membrane is smaller than the N1 membrane. This experimental observation has important consequences in terms of energy consumption in a waste water treatment plant.

c. Critical pressure and "elastic" pressure

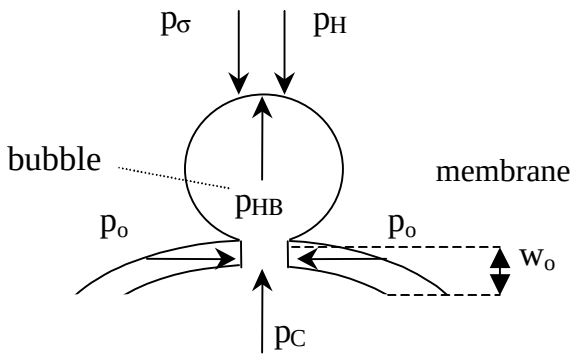

Figure 7: Balance of force during bubble formation at a flexible nozzle

The balance of force for a bubble formed at a flexible nozzle [3, 4] is described in Figure 7. In contrast to a rigid nozzle, the force due to the material elasticity has also to be taken into account. The required pressure to create a bubble (ΔP) is given by Eq. (12):

$$\Delta P > P_C - P_H + P_{HB} - P_\sigma - P_O \tag{12}$$

There is assumed to be no bubble spreading over the membrane. The hydrostatic correction for bubble height ($P_{HB} = \rho.g.r_B$) is negligible; the capillary pressure p_σ is equal to $4\sigma_L/D_{OR}$. The critical pressure ΔP_{Critic} to just initiate bubbling is identified as Eq. (13):

$$\Delta P_{Critic} = \frac{4\sigma_L}{D_{OR}} + P_O \tag{13}$$

The critical pressure is essentially a measured value, defined as the lowest pressure necessary to generate the first bubble. The ΔP_{Critic} values for the membranes are shown in Table 2. The critical pressure for the O1 membrane is smaller than that for the N1 membrane; this observation agrees with the ΔP =f (Q_G) results (Figure 6). Hence, it is possible to determine the "elastic" pressure P_O from Eq. (13) from the measured critical pressure and the associated hole diameter. The experimental P_O values are expressed in Table 2. The same conclusions as for the critical pressures are reached.

Membranes	**ΔP_{Critic}** (mbars)	**P_O** (mbars)
N1	38	26
O1	35	22

Table 2: Physical membrane properties

d. Deflection and flexibility

As an increasing pressure is applied, it causes the membrane to bulge: the membrane thus takes on the shape of a spherical cap (figure 7).

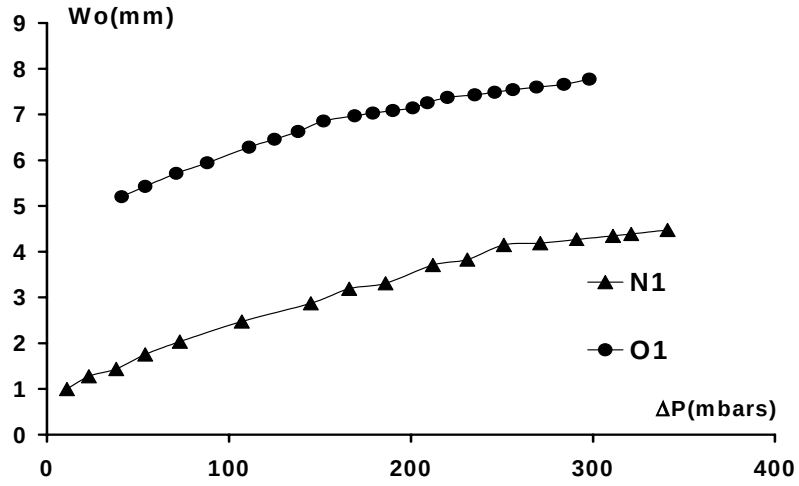

Figure 8: Membrane deflection at the pole versus applied pressure

Figure 8 presents the curves relating the membrane deflection at the pole W_O to the pressure drop. It can be observed that the deflection at the pole increases with pressure for all membranes. The deflection at the pole for the N1 membrane is smaller than that for the O1 membrane.

e. Theoretical approach for the membrane

The same approach as that of Loubière & Hébrard [5] is adopted in this part.

- **<u>The Rice & Lakhani model [2]</u>**

This model has been developed to show the connection between elastic and fluid mechanics in order to describe the membrane behaviour when it is subjected to pressure from below. The authors have shown that the excess tension T can be related to the applied pressure by Eq. (14):

$$T = K.\Delta P^n \qquad (14)$$

T is a function of the applied pressure, the deflection and the membrane radius and is given by the following equation:

$$T = \frac{\Delta P.Z^2}{4W_0} \qquad \text{when } W_O << Z \qquad (15)$$

$$T = \frac{\Delta P.Z^2}{4W_0} + \frac{\Delta P.W_0}{4} \qquad \text{when } W_O >> Z \qquad (16)$$

For each membrane, the K and n values for all membranes are presented in Table 3. Small values of K are associated with large deflections. The K values obtained with the N1 membranes are greater than those of the O1 membranes. In view of these results, it appears that the N1 membrane is less flexible than the O1 membrane.

The n values are related to the hole diameter and the n value for the N1 membrane is smaller than that of the O1 membranes. These results agree with the hole diameter and deflection measurements (Figure 4 and Figure 8).

Membranes	**$T = K.\Delta P^n$**		**$f = \alpha.Re^{\beta}$**		**G**	**f**
	K	n	α	β	(10^5 N/m^2)	Re=1000
N1	0.64	0.75	$8.62.10^4$	-1.39	20.98 (R^2 = 0.9806)	5.15
O1	0.23	0.81	$2.99.10^5$	-1.61	10.6 (R^2 = 0.9884)	4.82

Table 3: Theoretical approaches to characterize the membrane

- **<u>The Rice & Howell model [3]</u>**

Rice & Howell [3] have proposed a model to characterize the membrane behaviour with a shear modulus G defined by Eq. (17):

$$G = \frac{T_O}{2.b_o} \cdot \frac{1}{\left[1 - \frac{1}{\lambda_o^6}\right]} \qquad (17)$$

b_o is the membrane thickness. λo is the membrane extension ratio at the pole and is represented by the following equation:

$$\lambda_0 = 1 + \frac{W_0^2}{Z^2} \quad (18)$$

T_o is the membrane excess tension and is determined by Eq. (19):

$$P_C = \frac{2.T_0}{R} \quad (19)$$

P_C is the pressure in the gas chamber. The membrane is assumed to be a spherical cap and its radius R is calculated by the following equation:

$$R = \frac{Z^2 + W_O^2}{2.W_O} \quad (20)$$

The shear modulus G is determined by calculating the slope of the curves relating $To.\lambda o^6/2bo$ to λo^6. For all the membranes, the results are shown in Table 3. Large values of G are associated with small deflections. Table 3 shows that the largest and the smallest G values are obtained with the membranes N1 and O1 respectively. In view of these results, it appears that the N1 membrane is more rigid than the O1 membrane. These results agree with the deflection measurements (Figure 8) and the K values (Table 3).

- **<u>The relation between the discharge factor and the orifice Reynolds number</u>**

The applied pressure and the gas flow rate values (Figure 6) are translated into dimensionless numbers: the discharge factor f and the Reynolds number Re for the gas through the orifice. The relation between f and Re is expressed as Eq. (21):

$$f = \frac{2.\Delta P}{\rho_G.U_G^2} = \alpha.\mathrm{Re}^{\beta} \quad (21)$$

The discharge factor depends on the hole diameter and on the pressure drop. Small values of f are associated with a small pressure drop and with a large hole diameter.

For the two membranes, the f values at Re = 1000 and the α, β values are presented in Table 3. The f values obtained with the O1 membrane are lower than those with the N1 membrane.

In view of these results, the N1 membrane needs greater pressure than the O1 membrane. These results agree with critical pressure measurements (Table 2).

3.2 CHARACTERISATION OF THE BUBBLE PROVIDED BY A SINGLE ORIFICE

a. The relation between detached bubble diameter and gas velocity through the orifice

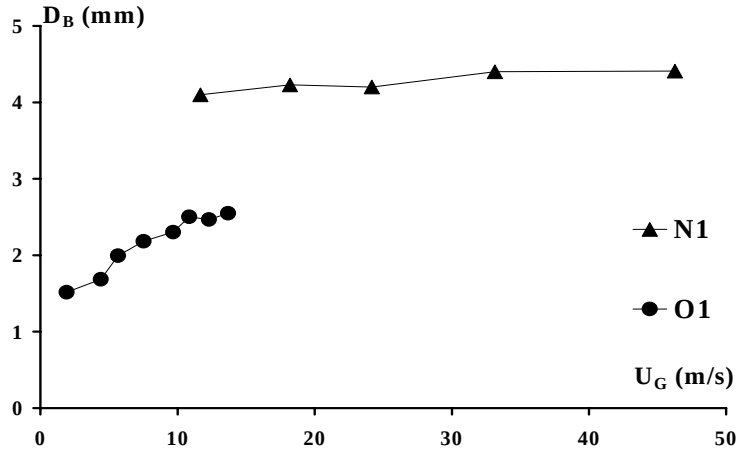

Figure 9: Bubble diameter at detachment versus gas velocity through the orifice for the membranes with a single orifice

Figure 9 shows the relation between the detached bubble diameter and the gas velocity through the orifice for the two membranes. For the O1 membrane, the bubble diameter increases less than linearly with the gas velocity through the orifice whereas the bubble diameter remains constant for the N1 membrane. The N1 membrane has a behaviour comparable to a rigid orifice [11]. For the O1 membrane, the bubble diameter curves presented in Figure 9 are classical for a flexible orifice [5].

Comparing the two membranes, the largest bubbles are produced with the N1 membrane whatever the gas velocity through the orifice: the N1 membrane generates bubble diameters two times greater than those of the O1 membrane. The difference in the bubble diameters

observed between these two membranes can be explained by the existence of a large inertial force in the case of the N1 membrane [11].

b. Relation between bubble formation frequency and gas velocity through the orifice

The bubble formation frequency curves as a function of the gas velocity through the orifice are given in Figure 10 for the two membranes.

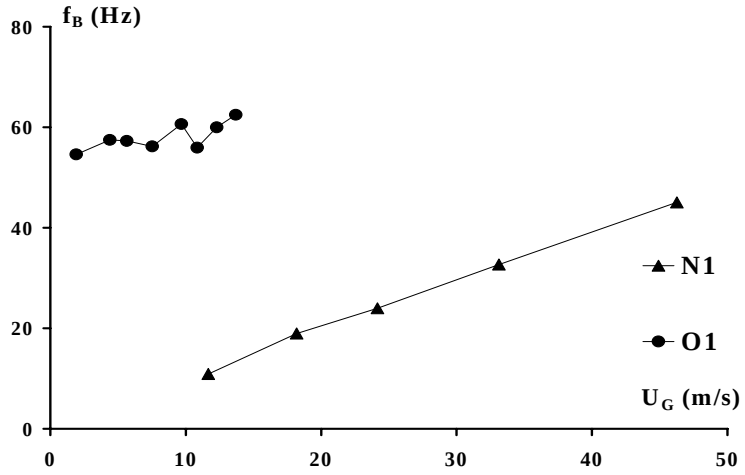

Figure 10: Bubble formation frequency versus gas velocity through the orifice for the membranes with a single orifice

Figure 10 shows that the bubble formation frequencies of the O1 membrane are greater than those of the N1 membrane. For the N1 membrane, the bubble frequency increases continuously with an increase in U_G, whereas it remains roughly constant for the O1 membrane.

According to Loubière et al [11], the N1 membrane has a behaviour comparable to a rigid orifice and the behaviour of the O1 membrane is classical for a flexible orifice.

4. COMPARISON OF THE MULTI-ORIFICE MEMBRANES

In order to see if the results obtained with a single orifice are maintained with multi orifices, the two membranes with four orifices were compared.

4.1 CHARACTERISATION OF THE MEMBRANES WITH MULTI ORIFICES

The following results are restricted to the measurements of the hole diameter, the pressure drop and the critical pressure.

a. Equivalent hole diameter

For the membranes with multi orifices, the same experimental method was used to measure the hole diameter as that used with the single orifice membrane. With the four orifice membrane, the hole diameters were measured when the four orifices are in function. The relations between hole diameter and gas velocity through the orifice for the membranes with four orifices, N4 and O4, are presented in Figures 11 and 12 respectively.

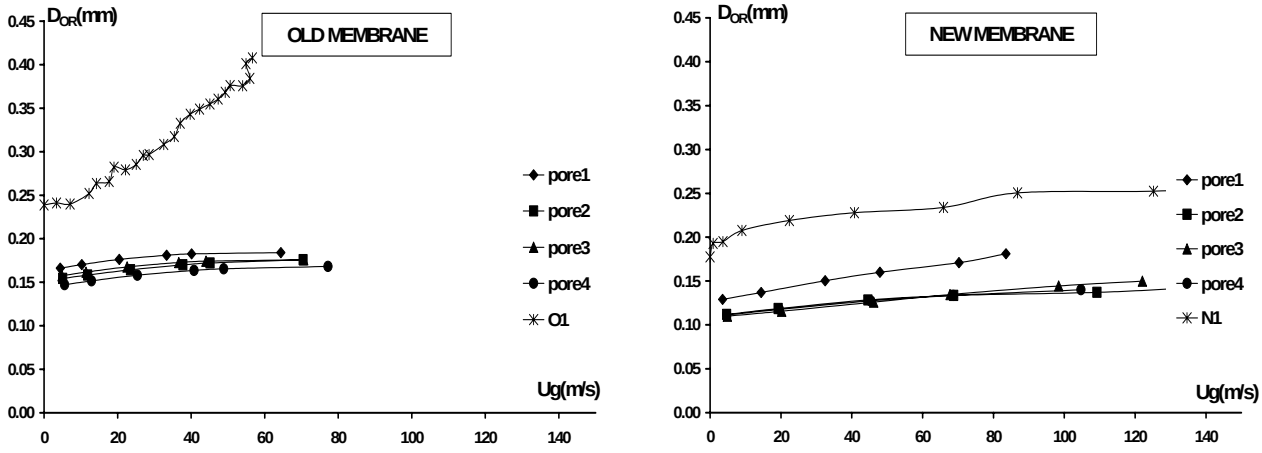

Figures 11 and 12: Equivalent hole diameter versus gas velocity through the orifice for the old and new membranes respectively (with a single orifice and for each orifice of the four orifice membrane)

For both membranes with four orifices, the apparent equivalent hole diameters for each orifice are very close: no significant difference appears between the four hole diameters. The variation of the hole diameter with the gas velocity through the orifice is less pronounced than with a single orifice membrane: just a slight increase is observed. The hole diameters of the new membrane with four orifices are close to those obtained with the old one. Moreover, the apparent equivalent hole diameters for the membranes with four orifices are significantly lower than those of the single orifice membranes.

b. Pressure drop and critical pressure

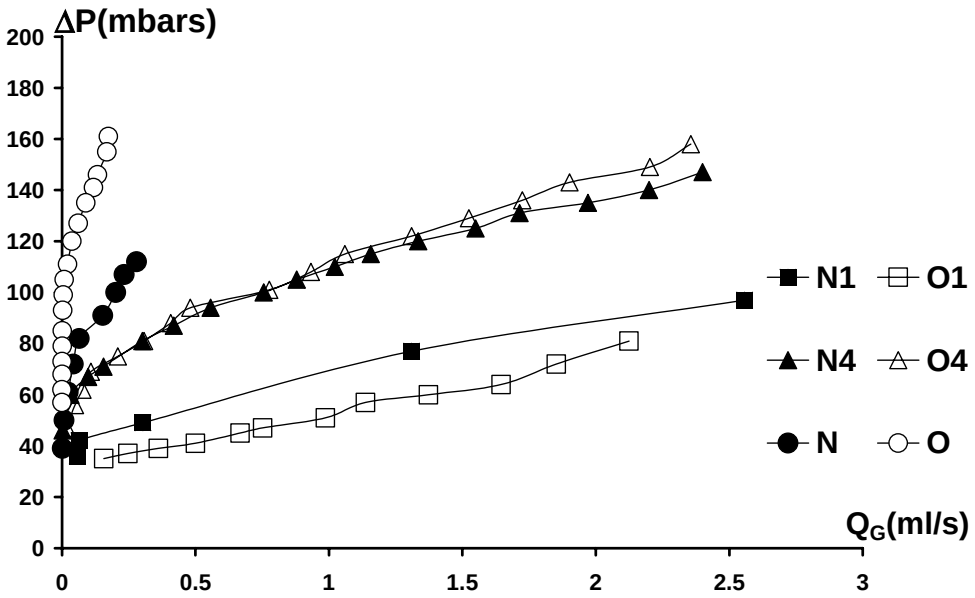

Figure 13: Pressure drop versus gas flow rate through the hole each orifice for all the membranes (single and multi orifices)

Figure 13 presents the experimental curves relating the pressure drop to the gas flow rate for the membranes with a single orifice (N1 and O1), with four orifices (N4 and O4) and with multi orifices (N and O). Whatever the membrane, the pressure drop increases with the gas flow rate. For a given gas flow rate, the pressure drops observed with four and multi orifice

membranes are larger than those with a single orifice membrane. The critical pressures for the N membrane and the O membrane are 35 mbars and 55 mbars respectively, and the critical pressure for the N4 and the O4 membranes are 49 and 62 mbars respectively. This observation agrees with the ΔP =f (Q_G) results presented in Figure 13: the new membrane with multi orifices creates lower ΔP values than the old one.

To explain the variation in ΔP for all the membranes, the expression of the gas velocity through the orifice (Eq. 11) and of the discharge factor (Eq. 21) are combined. The applied pressure drop can be derived as Eq. (22):

$$\Delta P = \frac{f.8.\rho_G.Q_G^2.}{(\pi.D_{OR}^2.N_{OR})^2} \tag{22}$$

For a given gas flow rate, the ratio of the pressure drop associated with two membranes can be deduced as Eq. (23):

$$\frac{\Delta P_1}{\Delta P_2} = \left(\frac{D_{OR2}^2.N_{OR2}}{D_{OR1}^2.N_{OR1}} \right)^2 \times \frac{f_1}{f_2} \tag{23}$$

According to Eq. 23, the pressure drop is a function of the hole diameter, the number of membrane orifices and the discharge factor. The hole diameter of the new and old membranes with four orifices are close in value and it can be assumed that the discharge factor are also close in value, by extrapolation from the calculation for the single orifice membrane. From these results, it seems probable that it is the rigidity of the membrane which causes its lower pressure drop values. In contrast, it is the hole diameter which mainly controls the ΔP values for the membranes with a single orifice since the discharge factor values obtained are similar for both membranes.

Regarding the ΔP values obtained with the membranes with multi orifices, the numbers of membrane orifices measured experimentally (210 and 270 orifices for the O and N

membranes respectively) become the parameters which determine the variation in the membrane pressure drop.

To explain the difference in critical pressure ΔP_{Critic} for the membrane, it is possible that the glue used to fill up the unwanted holes has changed the elastic membrane properties, particularly in the case of the four orifice membrane.

4.2 CHARACTERISATION OF THE BUBBLE PROVIDED BY THE MEMBRANES WITH MULTI ORIFICES

The bubble generation phenomenon has been studied only for the four orifice membrane.

a. The relation between detached bubble diameter and gas velocity through the orifice

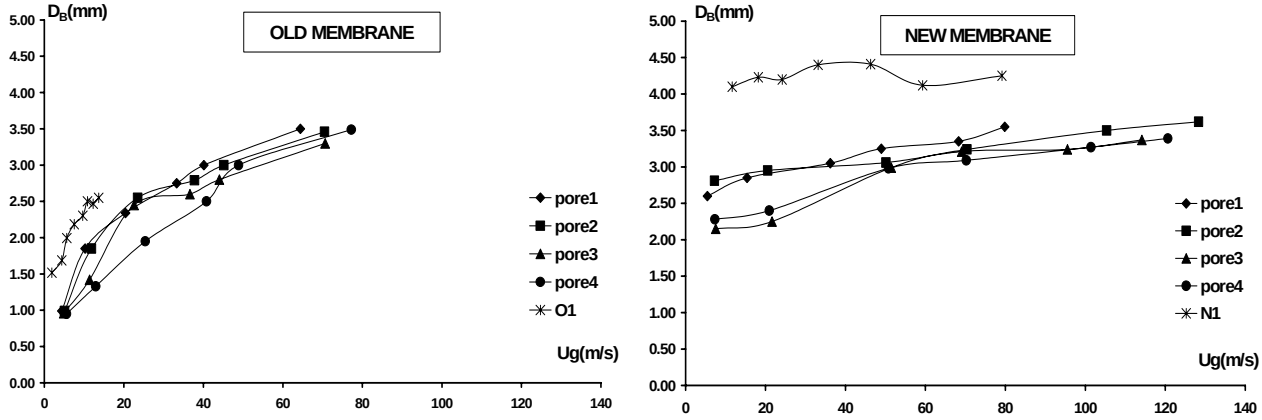

Figures 14 and 15: Bubble diameter at detachment versus gas velocity through the orifice for the old and new membranes respectively (with a single orifice and for each orifice of the four orifice membrane)

Figures 14 and 15 show the relation between the detached bubble diameter and the gas velocity through the orifice for the different types of membranes (the old and new membranes respectively). For the old membrane, the detached bubble diameters increase less than linearly

with the gas velocity through the orifice whatever the number of orifices. Also, the bubble diameters generated by the four orifices of the old membrane are smaller than those of the single orifice old membrane. According to Figure 15, the bubble diameters generated from the four orifices of the new membrane remain nearly constant with the gas velocity and are also smaller than the bubble diameters generated from the single orifice new membrane. In addition, the differences between the D_B values generated from a single orifice and from each orifice of the four orifice membranes are more pronounced at low Ug (below 40 m/s) than at high Ug (above 40-100 m/s). To conclude, it appears that the membrane behaviour (in terms of $D_B = f(Q_G)$) remains the same either with a single or four orifice membrane.

To study the membranes with multi orifices, the coalescence phenomenon at the level of the bubble formation becomes an essential factor to characterize the bubble diameters generated from the membrane and to evaluate their performance in terms of the bubble surface for mass transfer.

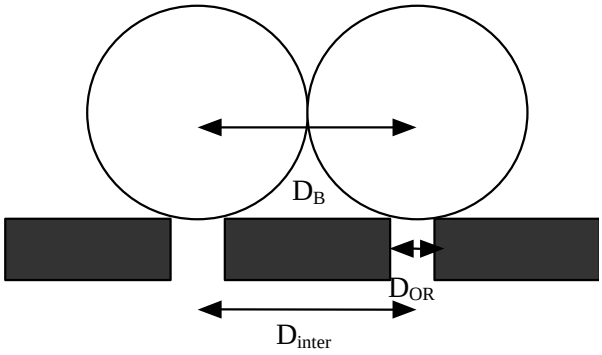

Figure 16: Critical condition for bubble coalescence

The inter-orifice distance is an important parameter when considering the coalescence phenomenon at the level of the bubble formation [12]. If the inter-orifice distance D_{inter} is larger than a critical value D_{CR}, then coalescence (at bubble formation) will never occur. On the contrary, if this distance is lower than the critical value, then coalescence might occur. It will definitely occur if the interaction time between bubbles is longer than the liquid film

drainage time. In this case, the bubbles grow approximately in phase and when two neighbouring bubbles reach a sufficiently large size to touch each other, the surface tension will no longer be sufficient to keep them as individual structures; the Van Der Waals intermolecular forces will also make them merge into a single large bubble.

The critical distance D_{CR} for two equally size bubbles to touch and to coalesce is the spherical equivalent diameter D_B, as sketched in Figure 16 and defined as:

$$D_{CR} = D_B = \sqrt[3]{\frac{6.V_B}{\pi}} \tag{24}$$

The critical distance ratio δ can also be defined as follows:

$$\delta = \frac{D_{\text{int}er}}{D_{CR}} \tag{25}$$

If the critical distance ratio δ is lower than one, coalescence during the bubble formation might occur. Whereas, if $\delta > 1$, the bubbles cannot coalesce during their growth.

Under the present operating conditions, some typical photographs of bubble formation generated from the new and the old membranes with four orifices are shown in Figure 17 (a) and (b) respectively.

(a) New membrane

(b) Old membrane

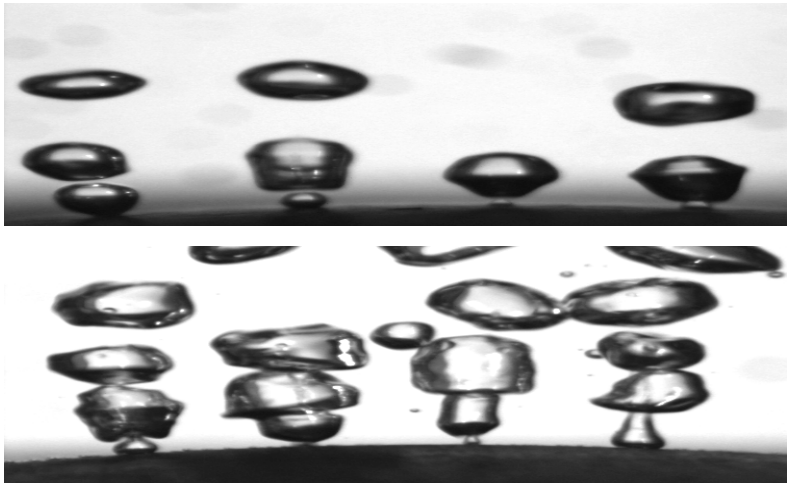

Figure 17: Typical Bubble formation photographs with a four orifice membrane (U_G = 125 m/s)

Although, the generated bubbles are not spherical, these images prove that under these conditions, no coalescence at the bubble formation occurs even for high U_G. These results agree with the inter-orifice distance D_{inter} (about 4.2 mm) measured experimentally and the detached bubble diameters (Figures 14 and 15).

b. Relation between bubble formation frequency and gas velocity through the orifice

Figures 18 and 19 show the relation between the bubble formation frequency and the gas velocity through the orifice for the new and old membrane respectively, with a single orifice and for each orifice of the four orifice membrane.

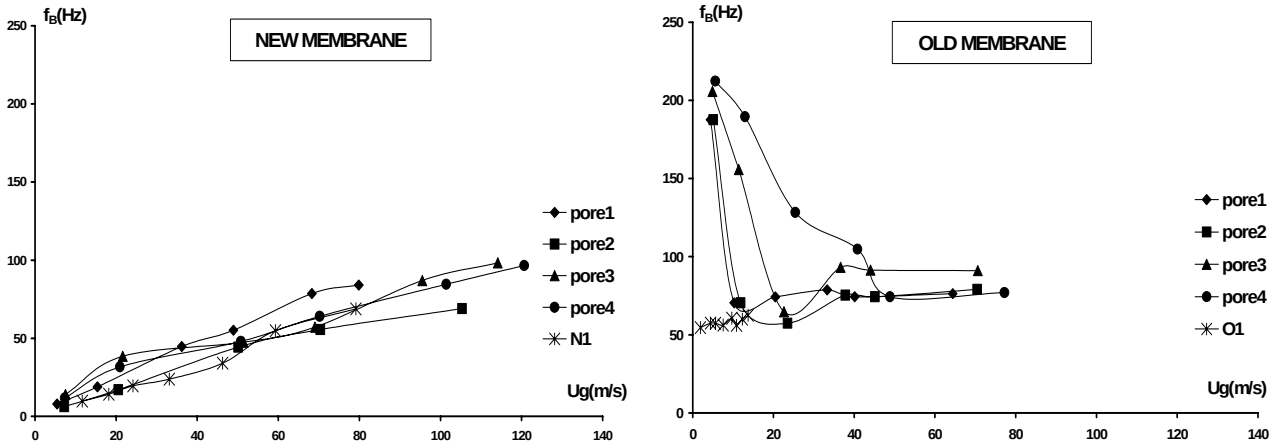

Figures 18 and 19: Bubble formation frequency versus gas velocity through the orifice for the new and old membranes (with a single orifice and for each orifice of the four orifice membrane)

For the new membrane with four orifices, the bubble frequency clearly increases with the gas velocity through the orifice for each orifice. These results agree with those observed with the new membrane with a single orifice. As shown in Figure 19, the bubble formation frequency associated with the four orifice old membrane reaches a constant value above a critical gas velocity through the orifice; these results are in accordance with to those of the old membrane with a single orifice. It can be concluded that the four orifice membrane behaviour (in terms

of f_B) is the same as that with a single orifice membrane. For a given bubble diameter, the different bubble frequencies obtained for the new and the old membranes should involve different gas hold-up (ε_g), volumetric interfacial area (a) and overall mass transfer coefficients (K_La).

5. PERFORMANCES OF THE TWO MEMBRANES

5.1 INTERFACIAL AREA

To compare the interfacial area of the two membranes, the ratio of the interfacial area associated with two membranes is calculated by Eq. 8. For this purpose, the variations in the detached bubble diameter (Figures 14 and 15) and in the bubble formation frequency (Figures 18 and 19) are used. The terminal bubble rising velocity has to be calculated but its influence on the interfacial area is less pronounced.

Figures 20 and 21 present the variation of the interfacial area with the gas velocity through the orifice for the new and old membranes with a single orifice and with four orifices.

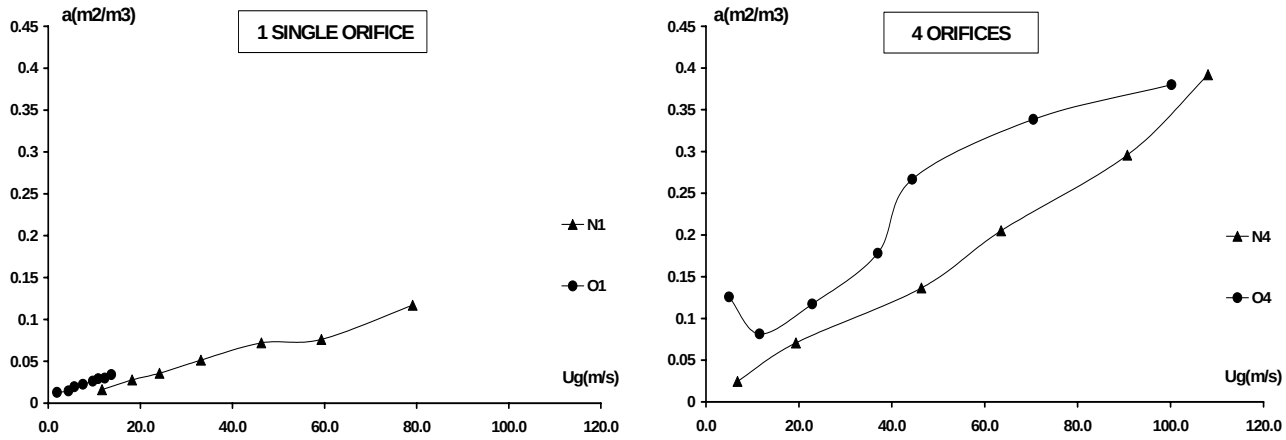

Figures 20 and 21: Volumetric interfacial area versus gas velocity through the orifice for the membranes with a single orifice and with four orifices respectively

These figures show that the interfacial area increases with the gas velocity through the orifice whatever the membrane. For the membrane with a single orifice, the interfacial areas of the old membrane are close to those obtained with the new membrane. The differences are more pronounced in the case of the membranes with four orifices: the interfacial areas for the old membrane are significantly greater than those of the new membrane. The present investigation demonstrates that the effects of the bubble formation frequency on the interfacial area are more marked than those of the detached bubble diameter.

5.2 POWER CONSUMPTION

The variations of the interfacial area with the power consumption for the membranes with a single orifice and with four orifices are shown in Figures 22 and 23 respectively.

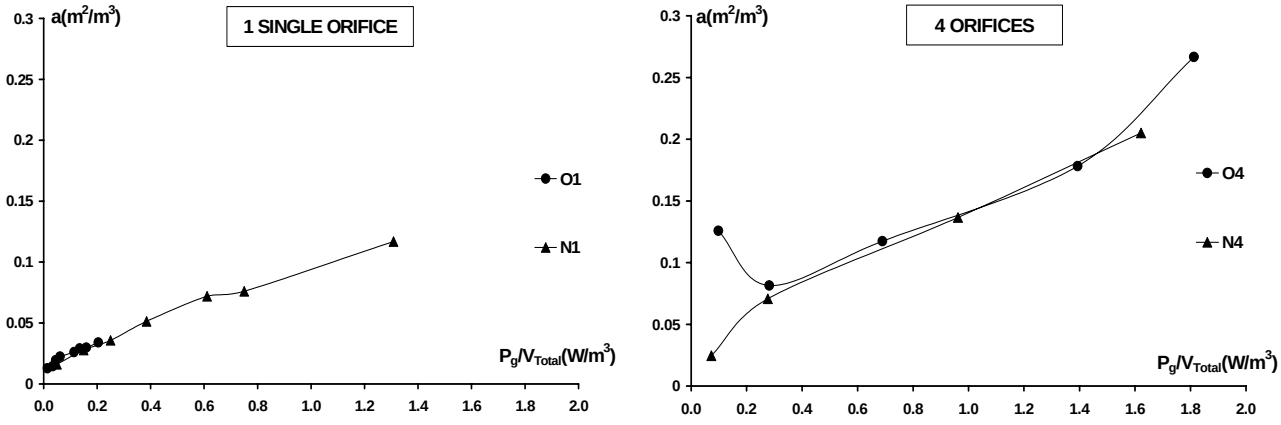

Figures 22 and 23: Interfacial area versus power consumption for the membranes with a single orifice and with four orifices respectively

According to these figures, the interfacial area increases with the power consumption. The variations of the interfacial area with the power consumption of the old membranes with a single and four orifices are close to those obtained with the new ones. Therefore, it can be concluded that for a given power consumption, the interfacial areas associated with the new

and the old membranes with a single and four orifices are similar. Moreover, for a given interfacial area, the power consumptions of the membranes with four orifices are less than those of the membrane with a single orifice.

According to the calculation of the membrane performances for both membranes, interfacial area measurements show that the two important parameters, the bubble diameter and the bubble formation frequency, compensate each other when comparing the new and old membranes. It is difficult to compare the global membrane performances (with all orifices) and to reach specific conclusions about them. Consequently, other parameters, such as the hole number and the membrane-operating lifetime, should be considered. Furthermore, the volumetric mass transfer coefficient (K_La) must be determined in order to understand mass transfer variation in terms of liquid-side mass transfer (K_L) and interfacial area (a).

6. CONCLUSION

The objective of this work was to compare two flexible membranes used in waste water treatment by ONDEO-DEGREMONT. For this purpose, the membranes with a single orifice and with four orifices were characterized in terms of: physical properties, bubble generation and membrane performances.

For the membrane with a single orifice, the results related to the physical properties and to the bubble generation have shown that:

- The applied pressure drop, the hole diameter and the deflection at the pole increase with gas flow rate.
- The pressure drops for the new membrane are greater than those of the old one.
- Whatever the gas velocity through the orifice, the hole diameters of the new membrane are lower than those of the old one.

- From the experimental and theoretical approach, the new membrane is less elastic (or more rigid) than the old membrane.
- Whatever the gas flow rate, the bubble diameter generated from the new membrane remains constant, whereas the associated bubble frequency increases continuously with an increase in U_G. These findings show that the new membrane has a behaviour comparable to a rigid orifice [11].
- The detached bubble diameter of the new membrane is larger than those of the old one, whereas the opposite behaviour is obtained in terms of bubble formation frequency.

The studies relating to the four orifice and the multi orifice membranes show that:

- The hole diameters of the membranes with four orifices are lower than those obtained with the membranes with a single orifice. The variation in hole diameter with the gas flow rate is less pronounced than with a single orifice membrane: just a slight increase is observed.
- For a given gas flow rate, the pressure drop observed with four and multi orifice membranes is larger that with a single orifice membrane.
- The pressure drop for the new membranes with four orifices and multi orifices is lower that of the old membranes. The rigidity of the new membrane causes the reduction in the pressure drop values, whereas the hole diameter is the parameter that controls the ΔP values for the membrane with a single orifice. Moreover, the number of the membrane orifices becomes the other important parameters which controls the pressure drop for the multi orifices membranes.
- No coalescence phenomenon at bubble formation is observed under these operating conditions, even for high U_G. This is explained by the inter-orifice distance being greater than the detached bubble diameters (the critical distance).

- In terms of the detached bubble diameter and bubble formation frequency, the membrane behaviours remain the same with multi orifices as with a single orifice.
- The detached bubble diameters from the membranes with four orifices are smaller than those obtained from the membrane with a single orifice. Nevertheless, the detached bubble diameters of the new membrane remain larger than those of the old one.
- Concerning the bubble formation frequency, there are no significant differences between the membranes with a single orifice or those with four orifices. The f_B of the new membrane remains smaller than that of the old one.

To compare the membrane performances, the interfacial area and the power consumption were determined. These results show that:

- The interfacial areas increase with the gas velocity through the orifice for both membranes. Also, for a given U_G, the interfacial areas of the new membranes with a single and four orifices are smaller than those of the old ones.
- For a given power consumption, the interfacial areas are close in value for both membranes.

This study has shown that the membranes used in industrial work can be characterized and can be compared by considering their physical properties, the bubble generation process and their performances. However, the hole number and the membrane operating life which is linked to its elasticity should also be taken into account when comparing membranes. The volumetric mass transfer coefficient (K_La) must be determined in order to understand mass transfer variation in terms of liquid-side mass transfer (K_L) and interfacial area (a).

Acknowledgements

This work has been carried out within the financial support of the ONDEO-DEGREMONT company (Croissy sur Seine, France). We would like to be grateful Bernard REBOUL for his technical support.

Notation

A	cross-sectional area of reactor	$[m^2]$
A_{OR}	hole area	$[m^2]$
a	interfacial area	$[m^{-1}]$
b_o	membrane thickness	[m]
D_B	bubble diameter	[m]
D_{CR}	critical distance between two orifices	[m]
D_{OR}	equivalent hole diameter	[m]
D_{inter}	inter orifice distance	[m]
f_B	bubble formation frequency	$[s^{-1}]$
G	shear modulus	$[N/m^2]$
g	acceleration due to gravity	$[m/s^2]$
H_L	liquid height	[m]
N_B	number of bubbles generated	[-]
N_{OR}	number of orifices	[-]
P_{atm}	atmospheric pressure	[Pa]
P_B	pressure inside the bubble	[Pa]

P_C	pressure in the gas chamber	[Pa]
P_H	hydrostatic pressure ($P_{atm} + \rho_L.g.H_L$)	[Pa]
P_{HB}	hydrostatic pressure for bubble height ($\rho_L.g.R_B$)	[Pa]
P_σ	pressure due to surface tension	[Pa]
P_O	pressure due to the membrane elasticity	[Pa]
P_g	power consumption in aerated liquid	[W]
ΔP	pressure drop created by the membrane sparger	[Pa]
ΔP_{Critic}	critical pressure	[Pa]
ΔP_{Total}	total gas pressure drop	[Pa]
q	gas flow rate through the orifice ($q=dV_B/dt$)	[m^3/s]
Q_G	gas flow rate	[m^3/s]
R	membrane (spherical cap) radius	[m]
S_B	total bubble surface	[m^2]
T	excess tension (Eq. 15-16)	[Pa.m]
T_B	bubble formation time	[s]
T_o	membrane excess tension (Eq. 19)	[Pa.m]
U_B	bubble rising velocity	[m/s]
U_G	gas velocity through the orifice	[m/s]
V_C	gas chamber volume between the control valve and the orifice	[m^3]
V_B	bubble volume	[m^3]
V_{Total}	total volume in reactor	[m^3]

W_O	membrane deflection at the pole	[m]
Z	membrane radius	[m]

Dimensionless numbers

f	discharge factor defined by $f = \Delta P/(1/2.\rho_G.U_G^2)$	[-]
Re	hole Reynolds number defined by $\mathrm{Re} = U_G.\rho_G.D_{OR}/\mu_G$	[-]

Greek symbols

α	constant from Eq. (11)	[-]
β	constant from Eq. (11)	[-]
δ	critical distance ratio	[-]
λo	membrane extension ratio at the pole	[-]
μ_G	gas viscosity	[Pa.s]
μ_L	liquid viscosity	[Pa.s]
ρ_G	gas density	[kg/m^3]
ρ_L	liquid density	[kg/m^3]
σ_L	liquid surface tension	[N/m]

References

[1] Rice R.G., Lakhani N.B., Bubble Formation at a puncture in a submerged rubber membrane, Chem Eng Commun, 24 (1983) 215-234.

[2] Rice R.G., & Howell S.W., Elastic and flow mechanics for Membrane spargers, AIChE Journal, 32 (8) 1986.

[3] Rice R.G., Tupperainen J.M.I, HEDGE R., Dispersion and hold up in bubble columns. Comparison of rigid and flexible sparger, Canadian Journal of Chemical Engineering, 59 (1981) 677-687.

[4] Bischof F., & Sommerfeld M., Studies of the bubble formation process for optimisation of aeration systems, Proceeding of the International Conference on Multiphase Flows, Tsukuba, Japan, September (1991) 24-27.

[5] Loubière K., Hébrard G., Bubble formation from a flexible hole submerged in an inviscid liquid, Chemical Engineering Science, 58 (2003) 135-148.

[6] Hébrard G., Bastoul D., & Roustan M., Influence of the gas spargers on the hydrodynamic behaviour of bubble columns, Trans IchemE, 74 (A) (1996) 406-414.

[7] Couvert A., Roustan M., & Chatellier P., Two-phase hydrodynamic study for a rectangular air-lift loop reactor with an internal baffle, Chemical Engineering Science, 54 (21) (1999) 5245-5252.

[8] Loubière K., Croissance et détachement de bulles générées par des orifices rigides et flexibles dans des phase liquides newtoniennes : Etude expérimentale et modélisation, Thèse N°663, INSA, Toulouse, France, 2002.

[9] Grace J.R. & Wairegi T.. Properties and Characteristics of drops and bubbles, Encyclopedia of Fluid Mechanics, Cheremisinoff. Chap 3, gulf Publishing Corporation, Huston, TX., (1986) 43-57.

[10] Bouaifi M., Hébrard G., Bastoul D., Roustan M., A comparative study of gas hold-up, bubble size, interfacial area and mass transfer coefficients in stirred gas-liquid reactors and bubble columns, Chemical Engineering and processing , 40 (2001) 97-111.

[11] Loubière K., Hébrard G. and Guiraud P., Dynamic of bubble growth and detachement from rigid and flexible orifices, Canadian Journal of Chemical Engineering, 81 (2003) 499-507.

[12] Pereira Dias M. I., Bubble formation at a multiple orifice plate submerged in quiescent liquid, Thèse, University Libre de Bruxelles Faculté des Sciences Appliquées, 1999